

## Surface Topography and Tunneling Spectroscopy in High-Temperature Superconducting Thin Films by Scanning Tunneling Microscopy†

R. T. Kao<sup>1</sup>, J. H. Horng<sup>1</sup>, S. J. Wang<sup>1</sup>, J. Y. Juang<sup>1</sup>, K. H. Wu<sup>1</sup>, T. M. Uen<sup>1</sup>,  
Y. S. Gou<sup>1</sup>, and T. H. Yang<sup>2</sup>

<sup>1</sup>*Institute of Electrophysics, National Chiao-Tung University,  
Hsinchu, Taiwan 300, R.O.C.*

<sup>2</sup>*Institute of Electro-Optical Engineering, National Chiao-Tung University,  
Hsinchu, Taiwan 300, R.O.C.*

(Received September 1, 1995)

The surface morphology and tunneling spectroscopies of the  $\text{YBa}_2\text{Cu}_3\text{O}_{7-x}$  (YBCO) and  $\text{TlBa}_2\text{Ca}_2\text{Cu}_3\text{O}_{9+x}$  (Tl-1223) high- $T_c$  superconducting thin films deposited on  $\text{LaAlO}_3(100)$  substrates were investigated by scanning tunneling microscopy (STM). The preliminary results show that although both systems have a common layer-like surface structure, the grain morphologies are quite different suggesting that they may follow different growth mechanisms probably due to the different preparation methods used. In addition, the tunneling current-voltage characteristics (IVCs) manifested features akin to that of charging effect-induced single electron tunneling in both systems. As a result, the gap-like structure observed in the  $dI/dV$ - $V$  curves may not be reflecting the superconducting energy gaps as commonly conceived.

PACS. 68.55.Jk - Structure and morphology; thickness.

PACS. 74.50.+r - Proximity effects, weak links, tunneling phenomena and Josephson effects.

PACS. 74.76.-w - Superconducting films.

Since the discovery of high- $T_c$  superconductors, many experimental techniques have been developed and employed to study the nature of the high- $T_c$  superconductivity. Among them, the electron tunneling measurements are considered to be advantageous for obtaining information about the fundamental properties of the high- $T_c$  superconductors [1]. In this respect, the scanning tunneling microscopy (STM) has been proven as a powerful tool for studying the surface topography, growth mechanisms [2,3] and surface electronic properties (e.g. energy gap, density of states) [4] of both superconducting thin films and crystals.

Indeed, in recent years, STM has been widely used to investigate superconducting materials, such as  $(\text{LaSr})_2\text{CuO}_4$  (LSCO) [5,6],  $\text{YBa}_2\text{Cu}_3\text{O}_{7-x}$  (YBCO) [7,8] and Bi-based cuprate [9,10] systems, and helped to gain rich insights in understanding these materials. However, relatively few studies have been performed on the Tl-based superconducting thin films, partly because of the difficulties suffered from making pure-phased samples.

† Refereed version of the contributed paper presented at the 1995 Taiwan International Conference on Superconductivity, August 8-11, 1995, Hualien, Taiwan, R.O.C.

In this paper, the surface morphology and tunneling spectroscopy of high-T, superconducting thin films of YBCO and Tl-1223 are compared by using STM. Our results show that, though the surface morphology in both systems have similar layer-like microstructure, the detailed structures of the individual grains are quite different, probably due to the different preparation methods used. In addition, the tunneling spectroscopies show clear evidences of Coulomb blockade and staircases on the I-V characteristics in both systems. These effects were first observed by Zeller and Giaever in 1969 [11] and were attributed to single electron charging effects. This particular observation implies that the surface tunneling characteristics obtained by the present STM configuration may not be directly associated with the superconducting energy gap as previously interpreted.

Both of the YBCO and Tl-1223 superconducting thin films used in this study were deposited on the single crystalline  $\text{LaAlO}_3$  (100) substrates. The YBCO films were deposited in-situ by KrF excimer laser ablation, whereas the Tl-1223 films were prepared by dc-sputtering with optimized post-annealing conditions. Details of the sample fabrication process were described elsewhere [12,13]. It is noted here that the zero-resistance transition temperatures  $T_{co}$ 's for the YBCO and Tl-1223 films are above 90K and 110 K, respectively. The transport critical current densities at 77K for both materials are all well above  $0^6 \text{ A/cm}^2$ , indicating the high quality of the samples.

The surface topography studies were performed by using a low-temperature STM system with a mechanically stripped PtIr tip. The constant current mode was operated at room temperature in air to obtain the image of the film surface. For tunneling spectroscopy measurements, a fixed bias voltage was applied to the tip at liquid nitrogen temperature while keeping the tip position fixed. For low temperature operations, the background pressure, which consists essentially the pure He gas, of the sample space was pumped to below  $10^{-2}$  torr to minimize He convection of He while keep enough heat exchange capability for temperature control.

Fig. 1 and Fig. 2 show the typical three-dimensional top view images of YBCO and Tl-1223 superconducting thin films, respectively. As is evident from the images, the surface morphologies of both material systems have very similar layer-like structure. However, the detailed structure of individual grains appears to be quite different. For the YBCO/ $\text{LaAlO}_3$  films, the grain structure displays clear stacks of terraces; a distinct signature of screw-dislocation mediated growth mechanism. Such results have also been observed previously for YBCO grown on YSZ (Yttria Stabilized Zirconia) substrates [14], indicating that they may follow a similar growth mechanism.

In contrast, as is evident in Fig. 2, the grain morphology of the Tl-1223 films appears to be more like striations rather than spirals. Since Tl-1223 films were prepared by single target dc-sputtering followed by post-annealing process, the superconducting phase was, therefore, formed from initially amorphous precursors instead of in-situ growth. As a result, the effect of film-substrate strain relief-induced dislocations may be less significant, leading to the absence of spiral morphologies. However, it is not clear at present how the striations formed. Whether it *is arisen from* the process alone or has anything to do with the nature of the materials has to be further investigated in a more systematic way.

Aside from the origins of the apparent difference in grain morphologies of these two materials, it is always interesting to see how the electronic properties are affected. Fig. 3 and Fig. 4 show the typical I-V and corresponding  $dI/dV$ -V characteristics obtained from

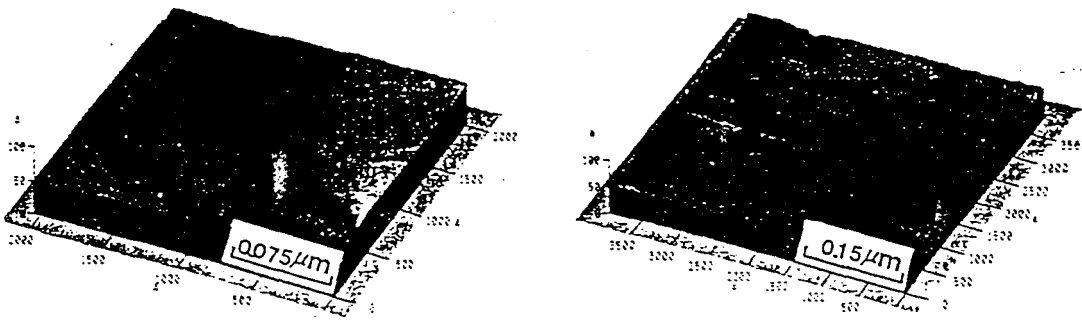


FIG. 1. The three-dimensional top view STM image of YBCO thin film. As is evident, the grain structure displays clear stacks of terraces.

FIG. 2. The three-dimensional top view STM image of Tl-1223 thin film. Notice that, the grain morphology appears to be more like striations rather than spirals.

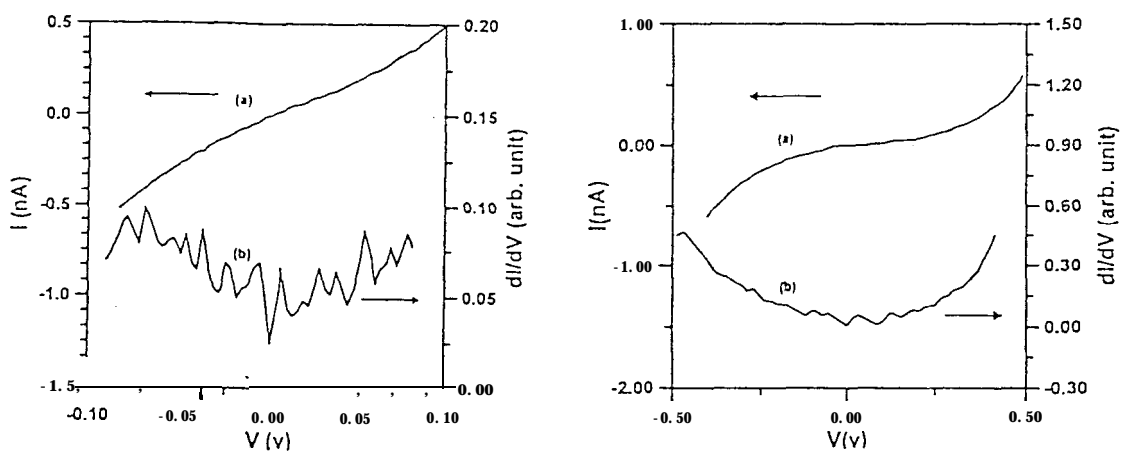


FIG. 3. (a) I-V characteristic of YBCO thin film at the fixed bias voltage  $V = -0.1$  v. (b) Directly derived conductance versus bias voltage curve from I-V data of (a).

FIG. 4. (a) I-V characteristic of Tl-1223 thin film at the fixed bias voltage  $V = -0.5$  v. (b) Directly derived conductance versus bias voltage curve from I-V data of (a).

electron tunneling taken on YBCO and Tl-1223 thin films, respectively. It is noted that for the present tunneling configuration, the electrons are tunneled from the PtIr tip to the superconducting films. As can be seen from curves(a) in both Fig. 3 and Fig. 4, although the steps were rounded noticeably by thermal noises ( $k_B T$ ), the step structure in the I-V curve is unambiguously observed. This is suggestive of the single electron tunneling (SET). The SET effect manifested itself a threshold voltage due to the Coulomb blockade charging effect, as depicted by the first zero-current step in the I-V curve show here. Indeed, by taking derivatives of both I-V curves and plotting as  $dI/dV$ -V, the multiple peaks structures signifying the typical Coulomb staircase structure are clearly evident, as shown on the two curves (b) in Fig. 3 and Fig. 4. We note that similar results have also been observed by van Bentum et al. [15]. In that study, a similar STM tip was used as the point contact on a granular Al/oxide/Al double junction system. The observed staircase structure was attributed to the ionization of a single impurity states existing in the oxide layer. Thus, it appears that, in the present tunneling structure (i.e. NIIS, where I and I' represent air gap and top surface layer of the film, respectively), the superconducting grains of both YBCO and Tl-1223 thin films may be regarded as that of granular Al layers.

We have also checked the temperature dependence of the position of the first peak in the  $dI/dV$ -V curves in both systems. The preliminary results showed that no dependence in the temperature rang of 4.2 K up to the transition temperature of respective materials. In fact, such structure remain observable even when  $T > T_c$ . This is suggestive that the peaks, especially the first one, may not be reflecting the energy gap of the superconductors. Further analysis in terms of single electron tunneling effect are currently underway to give a more quantitative understanding on these intriguing phenomena.

In summary, we have shown that, depending on the preparation method and the material system, the superconducting thin films grown on La.4103 (100) substrate can have very different grain morphologies. For YBCO films prepared by in-situ pulsed laser deposition, the films growth mechanism appears to be affected significantly by screw dislocations created due to strain-relief occurred when the film thickness exceeded some critical values. For post-annealed Tl-1223 films, on the other hand, growth striations were observed. The tunneling spectroscopies taken on both systems, however! suggest that the previously conceived gap-like multiple peak structure in  $dI/dV$ -V curves may just be manifestations of single electron tunneling, appeared as the observed Coulomb staircase structures demonstrated here.

This work was supported by the National Science Council of Taiwan, R.O.C., under grants No. NSC84-2112-M009-017-PH and No. NSC84-2112-M009-027-PH.

#### References

- [ 1 ] E. L. Wolf, *Principles of Electron Tunneling Spectroscopy* (1985).
- [ 2 ] M. E. Hawley, I. D. Raistrick, J. G. Beery, and R. J. Houlton, *Science*, 251, 1587 (1991).
- [ 3 ] D. G. Schlom, D. Anselmetti, J. G. Bednotz, R. F. Broom, A. Catana, T. Frey, Ch. Gerber, H. J. Guntherodt, H. P. Lang, and J. Mannhart, *Z. Phys.* B86, 163 (1992).
- [ 4 ] D. M. Ginsberg ed., *Physical Properties of High Temperature Superconductor III* ch. 7 (1992).
- [ 5 ] J. R. Kirtley, C. C. Tsuei, S. I. Park, C.C. Chi, J. Rozen, and M. W. Shafer, *Phys. Rev.* B35, 7216 (1987).

- [ 6 ] M. E. Hawley, K. E. Gray, D. W. Capone, and D. G. Hinks, *Phys. Rev.* B35, 7224 (1987).
- [ 7 ] J. Moreland, J. W. Ekin, L. F. Goodrich, T. E. Capobianco, and A. F. Clark, J. Kwo, M. Hong, and S. H. Liou, *Phys. Rev.* B35, 8856 (1987).
- [ 8 ] H. Haefke, H. P. Lang, G. Leemann, and H. J. Guntherodt, *Appl. Phys. Lett.* 60, 3054 (1992).
- [ 9 ] T. Hasegawa, M. Nantoh, and K. Kitazawa, *Jpn. J. Appl. Phys.* 30, L276 (1991).
- [10] Q. Chen and K. W. Ng, *Phys. Rev.* B45, 2569 (1992).
- [11] H. Z. Zeller and I. Giaever, *Phys. Rev.* 181, 789 (1969).
- [12] K. H. Wu, J. Y. Juang, C. L. Lee, T. C. Lai, T. M. Uen, Y. S. Gou, S. L. Tu, S. J. Yang, and S. E. Hsu, *Physica C*195, 241 (1992).
- [13] J. Y. Juang, J. H. Horng, S. P. Chen, C. M. Fu, K. H. Wu, T. M. Uen, and Y. S. Gou, *Appl. Phys. Lett.* 66, 885 (1995).
- [14] J. Y. Juang, R. T. Kao, M. C. Hsieh, H. H. Li, M. L. Chu, K. H. Wu, T. M. Uen, and Y. S. Gou, *Physica B*194-196, 385 (1994).
- [15] P. T. M. van Benthum, R. T. M. Smokers, and H. van Kempen, *Phys. Rev. Lett.* 60, 2343 (1988).